

# Upcycling waste commodity polymers into high-performance polyarylate materials with direct utilization of capping agent impurities

Received: 25 July 2024

Accepted: 4 March 2025

Published online: 12 March 2025

Cheng Li<sup>1,4</sup>, Guangming Yan<sup>2,4</sup>, Zhongwen Dong<sup>1</sup>, Gang Zhang<sup>2,3</sup>  & Fan Zhang<sup>1</sup> 

Commodity polymers are ubiquitous in our society, having replaced many inorganic and metal-based materials due to their versatile properties. However, their functionality heavily relies on the addition of various components known as additives, making it challenging to recycle the polymer fraction of plastic materials effectively. Thus, it is crucial to develop efficient chemical recovery strategies for commodity polymers and additives to facilitate the direct utilization of recovered monomers and additives without additional purification. Here, we develop a strategy for co-upcycling two types of waste commodity polymers, polycarbonate, and polyethylene terephthalate into polyarylate, a high-performance transparent engineering plastic. By incorporating a highly active metal-free ionic liquids catalyst for methanolysis and a two-stage interface polymerization technique with variable temperature control, we successfully prepare polyacrylate film materials from real end-of-life plastics with direct utilization of capping agent impurities in recovered monomers. These materials exhibit excellent thermal performance ( $T_g = 192.8^\circ\text{C}$ ), transmittance (reach up to 86.73%), and flame-retardant properties (V-0, UL-94), equivalent to those of commercial polyarylate (U-100, about \$10000/ton), and could be further easily close-loop recycled. Demonstrated in kilogram-scale experiments and life cycle assessments, this approach offers a low-carbon, environmentally friendly, and economically feasible pathway for upcycling waste commodity polymers.

Polymeric materials are indispensable materials for modern society and their current global annual production reaches up to 0.5 billion tons<sup>1</sup>. Unfortunately, most commodity polymers are discarded after first use and their recycling rate is sadly less than 15%, causing serious ecological and environmental problems as well as a significant waste of carbon resources<sup>2,3</sup>. Polyethylene terephthalate (PET) and polycarbonates (PC) are two kinds of the largest commodity polymers, highly demanded in packaging, automobile, textile and electronics

industry<sup>4,5</sup>. Currently, PET is mainly recycled through mechanical processes. However, this method requires sorting to obtain pure PET plastics and often leads to varying degrees of thermal and mechanical degradation<sup>6</sup>. In addition, discarded PC could slowly release Bisphenol A (BPA) under natural conditions, a compound widely acknowledged as both an environmental and human toxin with detrimental endocrine-disrupting effects, contributing to a growing environmental crisis<sup>7</sup>. Thus, the development of green and effective technologies for

<sup>1</sup>National Engineering Laboratory of EcoFriendly Polymeric Materials (Sichuan), College of Chemistry, Sichuan University, Chengdu, Sichuan, PR China.

<sup>2</sup>Institute of Materials Science and Technology, Analysis and Testing Center, Sichuan University, Chengdu, Sichuan, PR China. <sup>3</sup>State Key Laboratory of Polymer Materials Engineering, Sichuan University, Chengdu, PR China. <sup>4</sup>These authors contributed equally: Cheng Li, Guangming Yan.

 e-mail: [ganzhang@scu.edu.cn](mailto:ganzhang@scu.edu.cn); [fanzhang@scu.edu.cn](mailto:fanzhang@scu.edu.cn)

recycling commodity polymers, including PET and PC, has garnered significant attention<sup>8–10</sup>.

Recently, significant innovations have been achieved in chemical depolymerization and upcycling of waste PET and PC into high-valued chemicals. For example, through tandem catalysis, PET can be converted into p-xylene (PX)<sup>11</sup>, 1,4-cyclohexanedicarboxylate (DMCD)<sup>12</sup>,  $\beta$ -ketoadipate<sup>13</sup>. PC could also be upcycled to cycloalkanes for sustainable aviation fuels<sup>14</sup>, BPA-based oligoesters<sup>15</sup>. However, the upgrading efficiency of these strategies has not yet been deemed satisfactory for real end-of-life plastics. On the other hand, re-polymerizing the recovered monomers to materials with superior performance presents a more appealing alternative within the framework of a sustainable circular economy<sup>16–25</sup>. The solvolysis methods, such as hydrolysis, aminolysis, and alcoholysis, have been fully identified as the most effective chemical recycling technique to obtain monomers from these polyester materials<sup>26–33</sup>.

Despite advancements, persistent challenges exist, with the primary issue being the prevalence of diverse additives in end-of-life plastics<sup>34–37</sup>. These compounds, including softeners, antioxidants, colorants, flame-retardants, and capping agents, significantly complicate the efficient recycling and re-polymerization processes, impeding the viable transition of these materials into a second lifecycle<sup>1,17,24</sup>. Conventional practices involve separating additive impurities from recovered monomers through additional purification, leading to high energy consumption and costs (Fig. 1a). To date, there have been few reports on the use of additives in plastic recycling. Accordingly, it is imperative to develop efficient chemical recovery strategies for both commodity polymers and additives to facilitate the direct utilization of recovered monomers and additives without the need for additional separation.

Here, we present an effective method for co-upcycling PC and PET into polyarylate (PAR), as illustrated in Fig. 1b. PAR, a high-performance special engineering plastic, finds extensive applications across aerospace systems, automotive components and electronic devices due to its exceptional thermal resistance, robust mechanical characteristics, and remarkable light transmission capabilities<sup>38–40</sup>. By using the designed [TBDH]Ac catalyst, we were able to achieve a monomer yield of 98% and 99% in the methanolysis of PC and PET,

respectively. It is important to note that para-tert-butyl-phenol (PTBP) as a capping agent was found in the recovered BPA (r-BPA) obtained from various waste PC materials. In contrast to conventional practices to purify the monomers for further use, we designed a two-stage interface polymerization technique with variable temperature control (the first step polymerization temperature: 5–10 °C, the second step end-capping reaction temperature: 15–18 °C) to co-upcycling of PC and PET into recovered polyarylate (r-PAR) without extra purification procedure of BPA monomers recovered from the waste PC. The r-PAR exhibits excellent thermal stability and has achieved a V-0 (UL-94) flame retardant rating, with performance equivalent to commercial U-100. A life cycle assessment (LCA) has shown that this approach provides a feasible solution with minimal environmental impact for recycling plastics, in comparison to current waste management methods.

## Results

### Catalyst design and methanolysis of waste PET and PC to monomers

Metal-free ionic liquids (ILs) have emerged as highly promising catalysts for methanolysis, attributed to their regulable organic cations and inorganic/organic anions<sup>41</sup>. Initially, a variety of ILs with different anions and cations was synthesized to systematically investigate their potential as catalysts in PC methanolysis, as illustrated in Fig. 2a. Upon altering the anion of ILs, the results showed that [TBDH]Ac exhibited the highest catalytic activity. In contrast, those with anions of strong acids, such as [TBDH]TFA, had minimal catalytic activity, resulting in less than 2% monomers. This difference may be due to the fact that the conjugated anions of weak acids have improved nucleophilic properties for methanol. When the cation of ILs was changed, [TBDH]Ac consistently showed the highest catalytic activity.

As shown in Fig. 2b and Supplementary Fig. 1, the catalytic activity of [TBDH]Ac for polyester methanolysis exhibits a gradual increase as the reaction temperature rises. At 100 °C, the conversion of PC during methanolysis nearly reaches 100% after 4 h. Previous studies have demonstrated that the hydrogen bonds formed between ionic liquids and reactants facilitate the cleavage of C–O bond<sup>28,42–44</sup>. We examined the

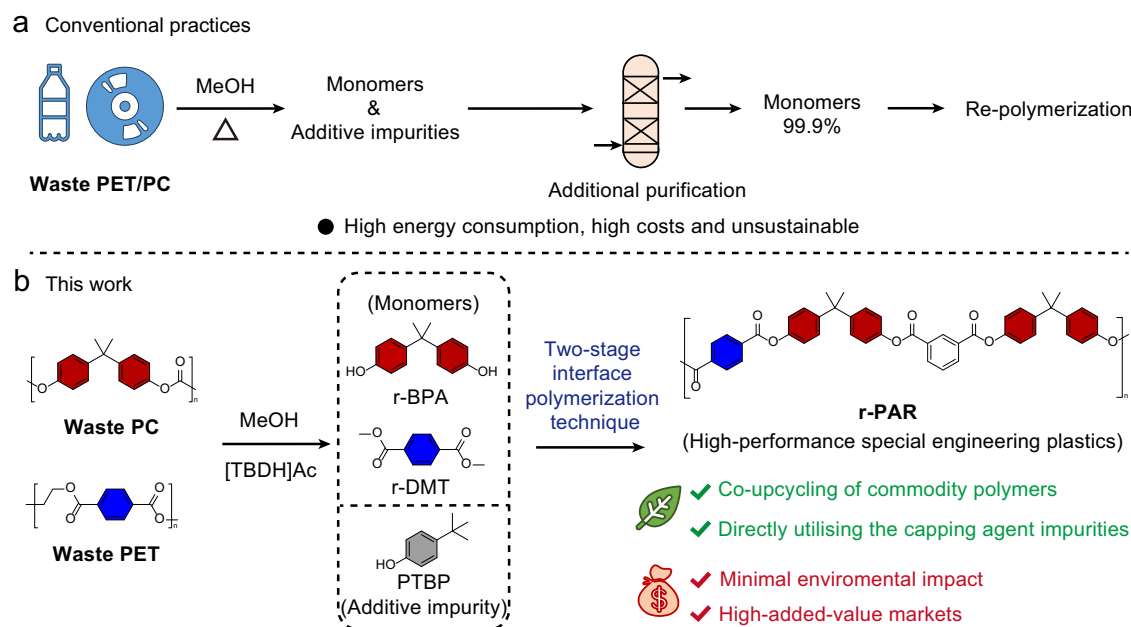


**Fig. 1 | Schematic of conventional and upcycling routes of waste PET/PC.**

**a** Conventional practices of chemical recovery of waste PET and PC, including solvolysis, purification and re-polymerization. **b** Our work is about the chemical

upcycling of PC and PET into r-PAR with direct utilization of the capping agent impurities. Recovered dimethyl terephthalate (r-DMT).

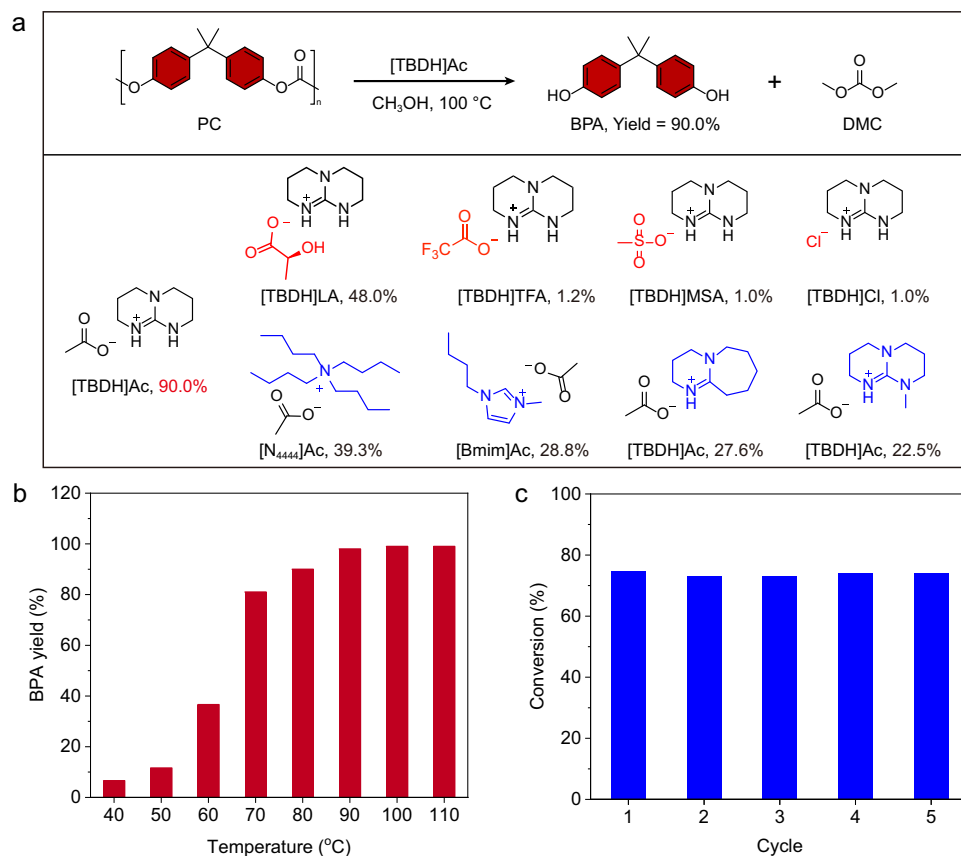


**Fig. 2 | Catalytic methanolysis of PC under mild conditions.** **a** Effect of the anions and cations of ionic liquids on PC methanolysis. Condition: catalyst (0.25 mmol), PC (0.5 g), MeOH (2 mL), 100 °C, 2 h. **b** The effect of temperature on PC methanolysis.

Condition: [TBDH]Ac (0.25 mmol), PC (0.5 g), MeOH (2 mL), 4 h. **c** Evaluation of the stability of [TBDH]Ac in PC methanolysis. Condition: catalyst (0.25 mmol), PC (0.5 g), MeOH (2 mL), 100 °C, 1.5 h.

activation of MeOH and PC using ILs through NMR spectroscopy, employing diphenyl carbonate (DPC) as a model compound for PC. The hydrogen bonding of the carbonyl group in DPC with [TBDH] was indirectly supported by the observed weakening of the electrostatic interaction between [TBDH] and the acetate ion ([Ac]), as indicated by chemical shifts 1 and 4 in Supplementary Fig. 2b. Additionally, when [TBDH]Ac was mixed with methanol, <sup>1</sup>H NMR spectroscopy further demonstrated significant hydrogen bonding between the hydroxyl group of MeOH and the acetate anion (see Supplementary Fig. 2c), indicating the methanol reactant was activated. These experiments indicate that [TBDH]Ac operates via a synergetic way, in which the acetate anion acts as a nucleophilic reagent to activate methanol, while the TBD cation functions as a hydrogen bond donor to activate the carbonyl group. It is essential to recognize that various factors can influence the chemical environment in solution, complicating the interpretation of results. A more comprehensive understanding of the mechanism necessitates additional in situ characterization and calculations.

The cyclic experiments revealed the remarkable stability of [TBDH]Ac, with its structure remaining unchanged after five runs (Fig. 2c and Supplementary Fig. 3). Additionally, the apparent activation energy ( $E_a$ ) for the reaction using [TBDH]Ac as the catalyst was determined to be 82.21 kJ mol<sup>-1</sup> (Supplementary Fig. 4). This methanolysis approach was highly efficient and eco-friendly as no additional toxic reagents, such as THF or CHCl<sub>3</sub>, were introduced.

We discovered that the [TBDH]Ac catalyst can also be used for PET methanolysis at 150 °C effectively (Supplementary Fig. 5) and applied it to real-life PET and PC wastes (Fig. 3a). For example, an experiment was conducted to convert 0.5 g of plastic mask (PET/PE) through methanolysis, resulting in 99% degradation of PET to obtain 0.45 g r-DMT (>99% purity) with 0.05 g unreacted polyolefin (PE). In the same way,

the system was also highly efficient in the selective degradation of PC waste in waste laptop shells and compact discs. After the reaction, acrylonitrile butadiene styrene plastic (ABS) and extra clad layer were separated by filtration, and the filtrates were then decolorized using activated carbon to obtain colorless r-BPA. However, the NMR spectroscopy indicated that the purity of r-BPA obtained from compact discs was approximately 98%, with an additional signal exhibited at 1.23 ppm in the spectroscopy (Fig. 3b and Supplementary Fig. 6). To confirm the identity of the unknown substance, GC-MS analysis was performed and it revealed that the substance was PTBP, which is also found in the r-BPA obtained from methanolysis of another commercial PC materials (Fig. 3c and Supplementary Fig. 7). The content of PTBP was found to be 2–4 mol% in these samples. Notably, the r-BPA extracted from laptop shells contained phenol instead of PTBP. The difference is likely due to the varying synthesis processes for PC. For example, the phosgene method introduces PTBP as a capping agent, while the melt polymerization method leads to residual phenol<sup>45,46</sup>. Consequently, the presence of additives in commercial PC is inevitable.

### Co-upcycling of waste PC and PET to PAR

The presence and the role of capping agents in r-BPA have often been overlooked or misidentified in existing research. However, it is a fact that these capping agents pose significant challenges to the re-polymerization of r-BPA<sup>47</sup>. We developed a two-stage interface polymerization technique to co-upcycle discarded discs (PC) and black fibers (PET) into r-PAR, without an extra purification procedure for BPA monomers recovered from waste PC (Fig. 4a). The polymerization temperature was initially controlled in the range of 5–10 °C, and then raised to 15–18 °C. The use of BPA sodium salt ensured excellent solubility at low temperatures, while the end-capping agent (p-tert

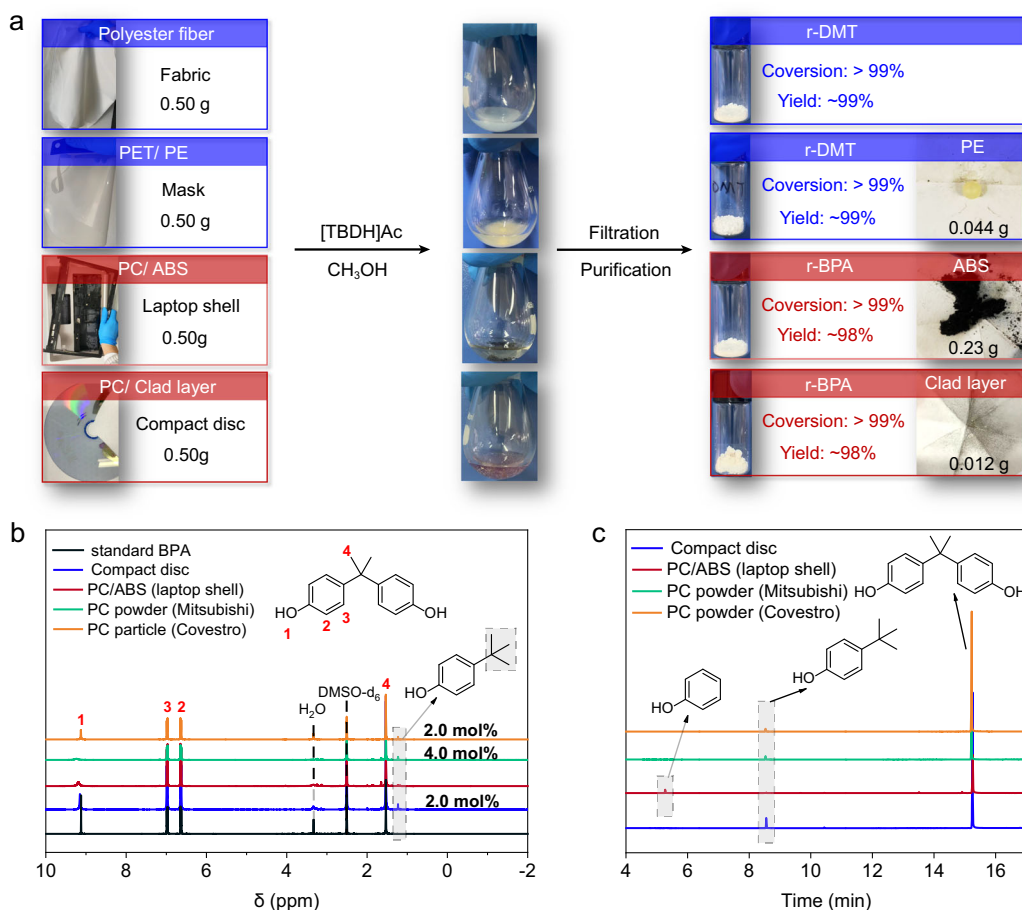


**Fig. 3 | Catalytic methanolysis of real-life waste PET and PC, and purity detection of recovered BPA monomers. a** Methanolysis of end-of-life waste PC and PET to monomers. Condition: [TBDH]Ac (0.25 mmol), waste plastic (0.5 g),

MeOH (2 mL), 100 °C (PC) or 150 °C (PET), 4 h. **b** <sup>1</sup>H NMR spectra of standard BPA and r-BPA recycled from various waste PC. (DMSO-d<sub>6</sub>, 400 MHz). **c** GS-MS of r-BPA recycled from various waste PC.

butylphenol), which is poorly water-soluble at low temperatures due to the presence of the tert-butyl group, effectively eliminated the impact of the capping agent on the initial polymerization (Supplementary Fig. 8a). In the absence of variable temperature control, r-PAR could not be successfully synthesized due to the adverse effect of PTBP on the polymerization reaction. (Supplementary Fig. 8b). After 3–4 h when the polymerization reaction was completed, we raised the temperature to dissolve the capping agent, direct utilization of capping agent impurities to allow the end-capping reaction (Fig. 4b). This approach effectively mitigates the influence of capping agents within r-BPA as impurities during the initial polymerization process, while concurrently harnessing their stabilizing effect of capping agents on polyarylate comprehensive performance.

The successful synthesis of PAR was confirmed by <sup>1</sup>H NMR and FT-IR spectra (Fig. 4c, d), which are mostly the same as the commercial PAR sample, U-100. In the FT-IR spectrum, a new absorption band near 1737 cm<sup>-1</sup>, attributed to the -COO- unit, was observable. That suggested the hydroxyl group had reacted with di-benzoyl chloride. Additionally, the disappearance of the hydroxyl (-OH) peak absorption at 3500 cm<sup>-1</sup> indicated the successful capping effect of residual PTBP in r-BPA. Importantly, we used capping agent impurities in situ rather than introducing them additionally. The inherent viscosity and average molecular weight ( $M_w$ ) of the synthesized r-PAR were 0.53 dL g<sup>-1</sup> and 4.32 × 10<sup>4</sup> g/mol, respectively, which are also similar to U-100. Considering the content of the capping agent may significantly influence the two-stage polymerization method, we further investigated the effect of PTBP in the range of 2–5% (Supplementary Fig. 9). As shown in Supplementary Table 1, the  $M_n$  of the produced PAR ranged from 1.38

to 1.77 × 10<sup>4</sup>, while the  $M_w$  was approximately 4.91 to 6.38 × 10<sup>4</sup>. These results indicate that the two-stage interface polymerization technique is effective across a relatively wide range of capping agents remaining within r-BPA.

We first conducted a comparison of the thermal properties of the synthesized r-PAR with PC and U-100 using DSC and TGA under nitrogen (Fig. 4e and Supplementary Fig. 10). The  $T_g$  of the resulting r-PAR and U-100 both ranged around 193 °C, which is approximately 49 °C higher than that of PC. From the TGA curve, it was evident that the initial thermal degradation temperature of r-PAR was also close to that of U-100 ( $T_d$  = 470 °C), demonstrating the prepared r-PAR from waste PET and PC exhibited similar thermal stability to the commercial PAR product. The mechanical properties of the r-PAR were further tested at room temperature using an electronic universal testing machine (Supplementary Table 2 and Supplementary Fig. 11). The tensile strength was found to be high, measuring up to 67.49 ± 0.77 MPa. It was quite close to those of U-100, and they were significantly higher than those of PC. The melt processability of a high-performance special engineering plastic is crucial for its widespread application. To assess the melt processability of the resulting resin r-PAR, the complex viscosities were studied using a parallel plate rheometer. (Fig. 4f). The complex viscosities of r-PAR ranged from 8200 to 2800 Pa s at temperatures between 280 °C and 320 °C, showing a decreasing trend as the temperature rose. This indicates that the resulting r-PAR, derived from waste PC and PET, has better melt flowability compared to U-100 at lower temperatures and similar melt flowability at 310–320 °C. This property is highly beneficial for the subsequent molding process of the resin.



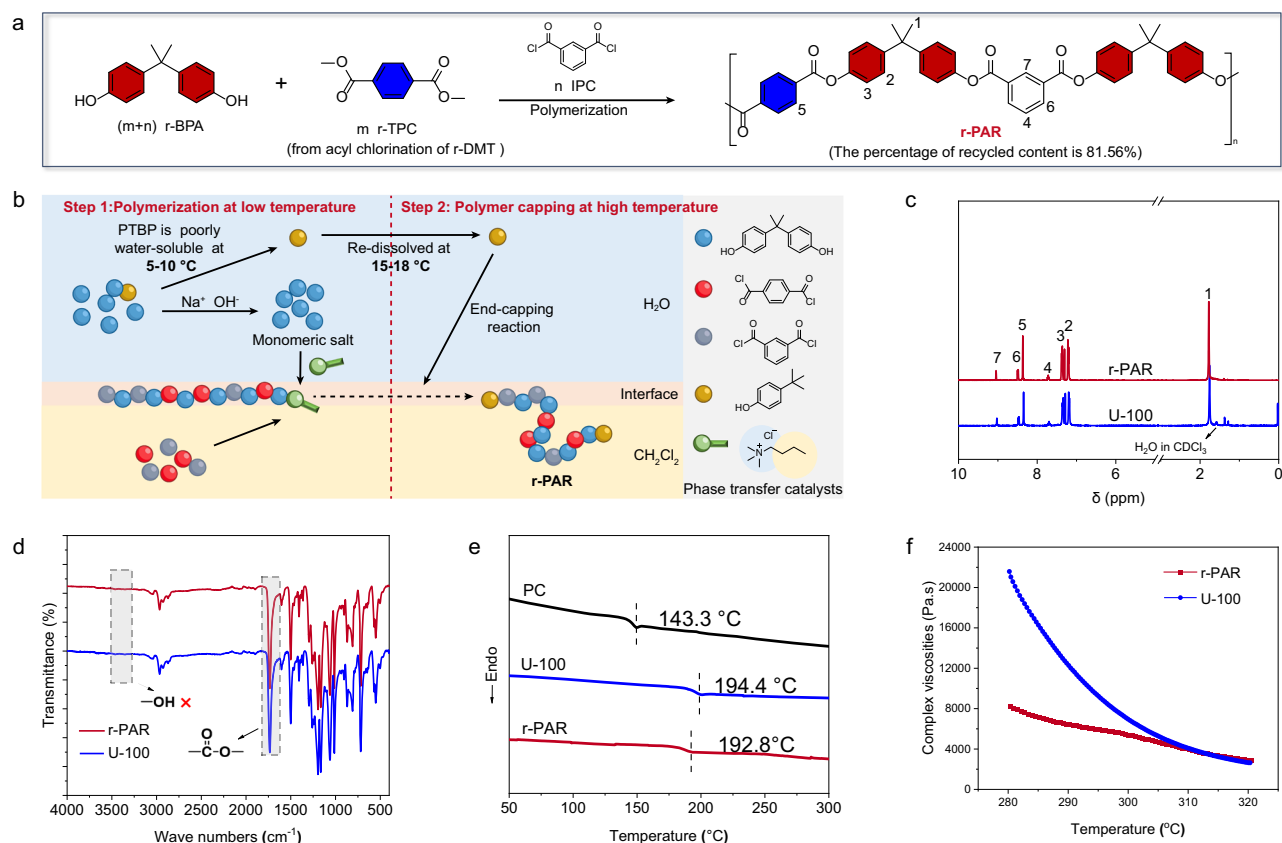


**Fig. 4 | Co-upcycling of waste PC and PET to high-performance special engineering plastics-polyarylates.** **a** Schematic reaction pathway for co-upcycling of waste PC and PET into r-PAR. The percentage of recycled content (RC) is calculated as follows:  $\text{RC} = \sum m(\text{C}, \text{H}, \text{O}) / M(\text{r-PAR})$ , where  $\sum m(\text{C}, \text{O}, \text{H})$  is the sum of the masses of the elements recovered from the waste plastic in the structural unit and  $M(\text{r-PAR})$  is the relative molecular mass of a structural unit of r-PAR. Recovered

terephthaloyl acid chloride (r-TPC); isophthalic acid chloride (IPC). **b** Schematic diagram for two-stage interface polymerization technique with variable temperature control. **c**  $^1\text{H}$  NMR spectra of r-PAR and U-100 ( $\text{CDCl}_3$ , 400 MHz). **d** The FT-IR spectra of r-PAR and U-100. **e** The DSC curves of various polymers at a heating rate of  $10\text{ }^{\circ}\text{C min}^{-1}$  in  $\text{N}_2$  atmosphere. **f** Plots of complex viscosities vs temperature of r-PAR and control sample U-100.

Following successful small-scale experiments, we moved on to conducting larger kilogram-scale experiments using a specially designed 10 L mechanically stirred reactor (Fig. 5a), and experimental details are shown in Supplementary Fig. 12 and Supplementary Table 3. In a typical experiment, we degraded 2.5 kg of laptop shells and recovered about 1.14 kg of BPA and 1.1 kg of ABS. Following this, we successfully carried out methanolysis of 1 kg of black polyester fabric. The selection of black polyester, which contains dyes, is more representative of practical applications than white polyester fabric; therefore, we opted for this material for our large-scale testing. The monomers recovered from these processes are then used to synthesize r-PAR and further produce PAR film materials with excellent transparency and flexibility. The films were detected by UV-vis. As demonstrated in Fig. 5b, the transmittance of the r-PAR film at 400 nm and 450 nm can reach up to 85.46% and 86.73%. It is observed that the r-PAR has superior optical properties and the transparency is comparable to that of commercial product U-100. Subsequently, the flame retardancy of r-PAR film materials was examined using the vertical burning test (UL-94)<sup>48</sup> to measure burning time after two ignitions and droplet behavior (Fig. 5c). PC samples burned ( $t_1 + t_2 = 7.6$  s) and produced molten polymeric droplets. This suggests that droplet damage occurs when PC is ignited, and the test ratings for PC are V-1 levels. In contrast, r-PAR exhibited different burning behavior compared to PC, with significantly reduced droplet hazards. The average after flame time ( $t_1 + t_2$ ) was only 2.8 s, and the test ratings are V-0 levels, indicating the highest flame-retardant levels for r-PAR.

Moreover, the r-PAR was also synthesized from waste CDs and black fabrics in a large-scale test (Supplementary Fig. 13). The thermal

stability of r-PAR-CD film material, with a glass transition temperature ( $T_g$ ) of 192.3  $^{\circ}\text{C}$ , is comparable to that of the r-PAR samples produced on a laboratory scale. Additionally, it exhibits excellent transmittance and flexibility. Finally, we also conducted methanolysis of r-PAR in large scale (Supplementary Figs. 14–16) and then re-polymerized the monomers to r-PAR-2, with its  $^1\text{H}$  NMR spectrum identical to that of r-PAR as illustrated in Supplementary Fig. 17. This process represents closed-loop recycling of PAR (Fig. 5d). These experimental results highlight the industrial potential of this chemical upcycling technology on waste commodity polymers.

### Life cycle assessment and input–output analysis

We applied a life cycle assessment (LCA) to compare the global warming potential (GWP) of our upcycling method with other existing plastic management methods. The system boundary of this LCA is set as cradle-to-gate, which is production-use-disposal. In our study, multiple paths were considered (Fig. 6a and Supplementary Fig. 18), including current waste management models (virgin PC, virgin PET, virgin PAR) and chemical recycling processes (co-upcycling of PC and PET into PAR and closed loop recycling of PAR). The process parameters were determined through kilogram-scale experiments, and additional details can be found in Supplementary Tables 4–9. Based on the carbon footprint, several scenarios were analyzed (Fig. 6b). The cumulative GWP of commercial plastics is as high as 9190  $\text{kg CO}_2 \text{ t}^{-1}$  under current waste management models (Path 1+2). When co-upcycling PC and PET into r-PAR (Case 1), the  $\text{CO}_2$  emissions were as low as 6320  $\text{kg CO}_2 \text{ t}^{-1}$ , leading to a 26% decrease in total GWP on a cradle-to-grave scope. Additionally, the GWP of virgin PAR was up to

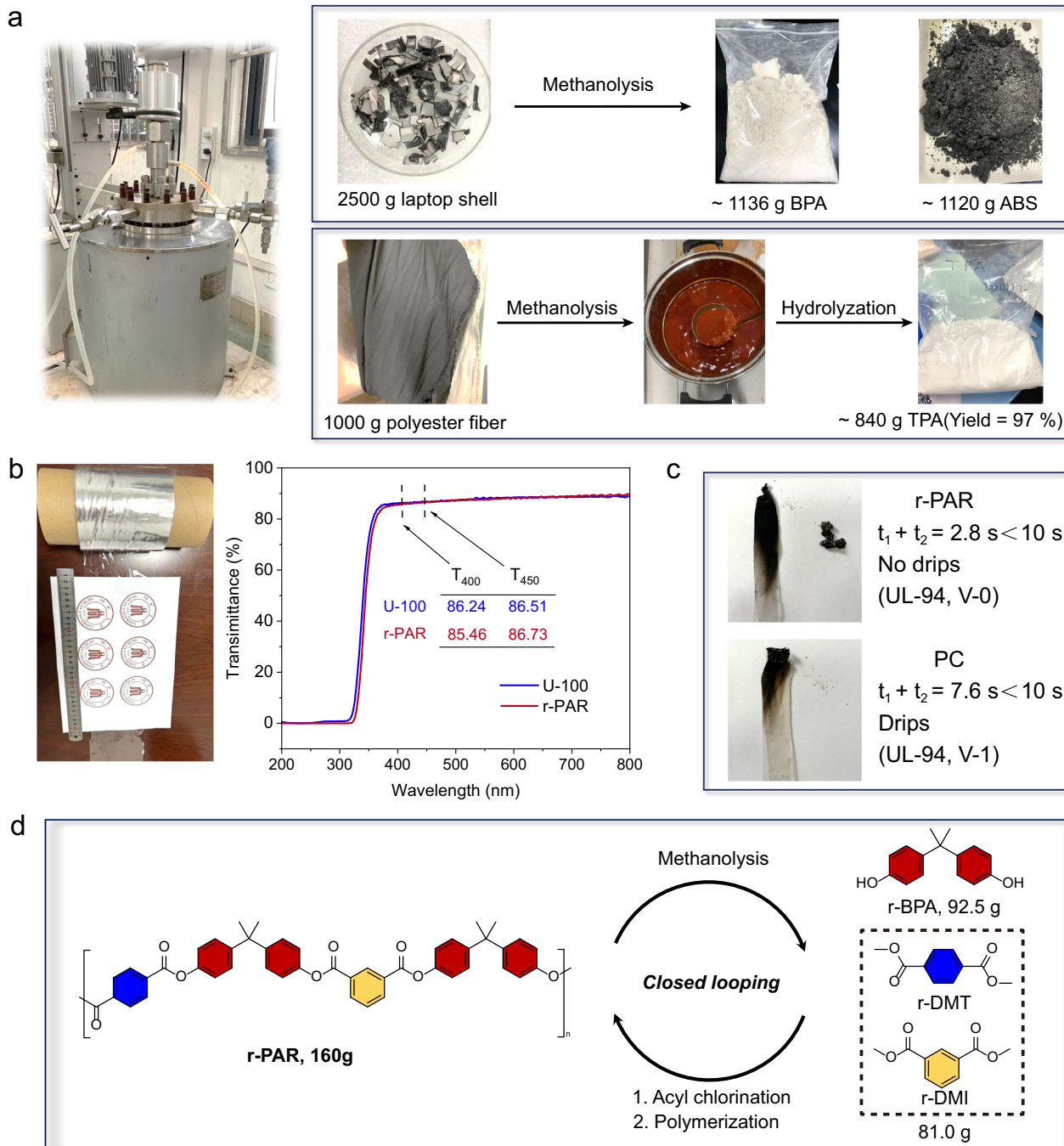


**Fig. 5 | Laboratory demonstration of larger-scale co-upcycling waste commercial plastics and fibers into r-PAR and its closed-loop recycling as well as the transparency and flame-retardancy test of the r-PAR film materials.**

**a** Digital images for the 10 L high-pressure reactor, commercial waste polymer reactants, and products based on the kilogram-gram scale methanolysis and

hydrolyzation experiments. **b** Digital image of the r-PAR film and the UV-vis spectra of r-PAR film and reference sample U-100 films. **c** Flame retardancy test results of r-PAR and PC stripes. ( $t_1 + t_2$ : average after flame time). **d** Schematic reaction pathway for closed-loop recycling of r-PAR.

8550 kg CO<sub>2</sub> t<sup>-1</sup> (Path 3), which is also an obvious burden for reducing CO<sub>2</sub> emissions. Compared with Path 3, the CO<sub>2</sub> emissions of closed-loop recycling of PAR were reduced by 15% (Case 2). Thus, recycling waste plastics as a resource to prepare new polymers has significant carbon reduction benefits. Meanwhile, we applied an LCA to compare the environmental impacts of the co-upcycling method with the existing method for handling fossil-based PC (Fig. 6c). Sadly, the current management of waste PC (Path 1) has a significant impact on freshwater ecotoxicity and human toxicity, particularly regarding cancer effects. Recycling substantially reduced the human toxicity

impacts (Case 1) by approximately 53%, attributed to the recycling of the toxic compound BPA. Compared to virgin PC, both the co-upcycling of PC and PET into PAR (Case 1) and closed-loop recycling of PAR (Case 2) reduced their impacts on freshwater toxicity, reducing freshwater toxicity by over 37%. Consequently, the strategies we propose offer sustainable solutions with a lower environmental impact.

The economic assessment of designated waste plastics recycling technologies is an imperative endeavor<sup>49,50</sup>. An input-output analysis of end-of-life PC and PET co-upcycling into PAR is presented in Fig. 6d as a Sankey diagram. Co-upcycling of commodity polymers generates

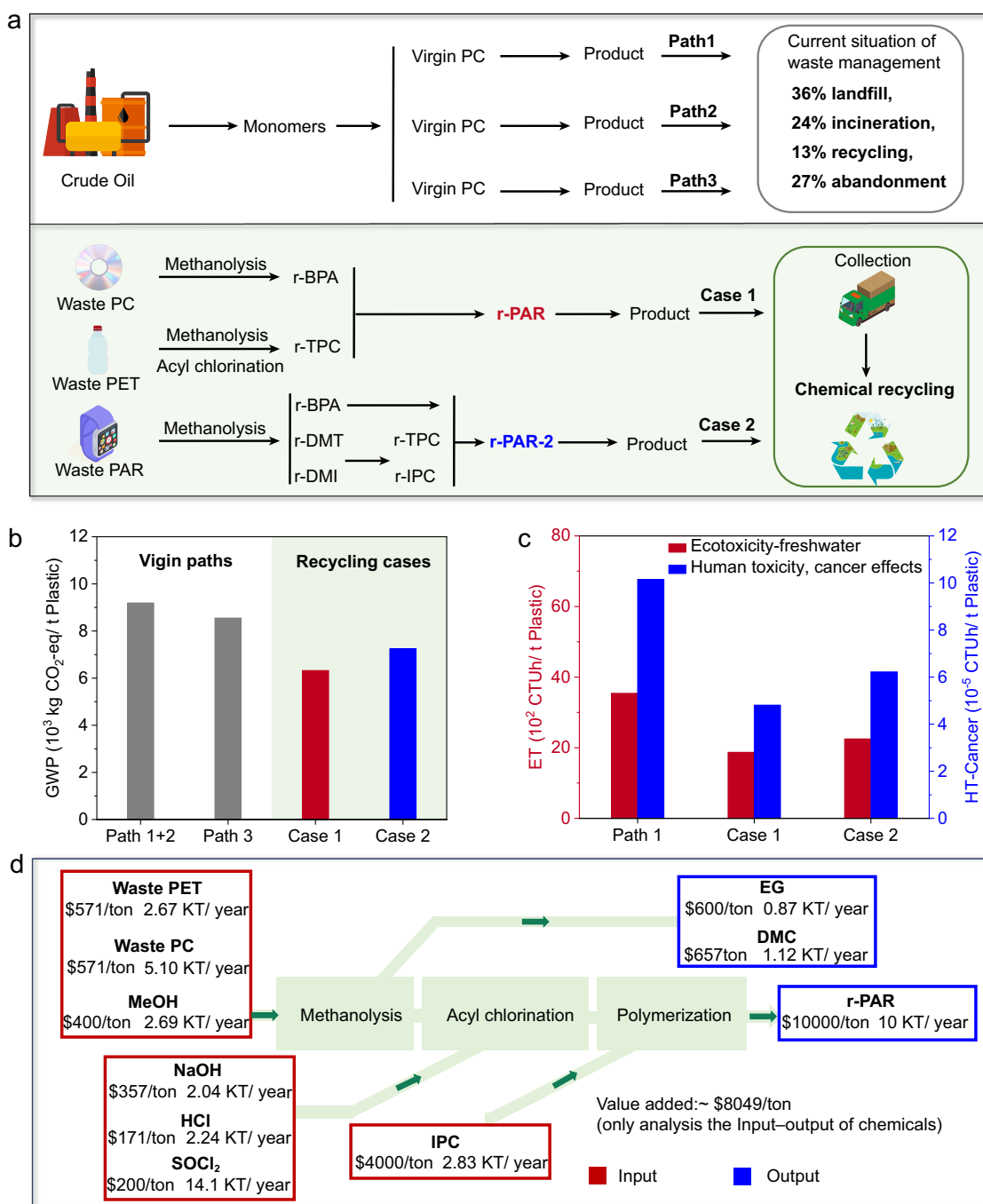


**Fig. 6 | The LCA and input-output analysis of co-upcycling waste PE and PC as well as the LCA of closed-loop recycling of PAR. a** The schematic diagram for current waste management and chemical recycling. The system boundary is cradle-to-grave. Comparison of **b** global warming potential and **c** ecotoxicity and human

toxicity in different routes for recycling post-consumer plastic. **d** Input-output analysis and market price for the production of r-PAR, EG, and DMC from waste plastics. KT, thousand metric tons. Recovered dimethyl isophthalate (DMI).

high-performance special engineering plastics, which use methanolysis, acyl chlorination, and polymerization that produces r-PAR, ethylene glycol (EG), dimethyl carbonate (DMC), etc. We configured r-PAR to achieve an annual throughput of 10,000 tons and conducted a thorough economic assessment by analyzing the mass accounting and prices of key chemicals, including TPC, EG, DMC, etc. For r-PAR, we propose the same selling price of \$10,000 per ton as commercial PAR (U-100) as the performance of r-PAR is comparable to that of commercially available U-100 with the added benefit of low carbon emissions. In our input-output analysis, we found that the value added per ton of recovered PAR produced is as high as \$8049. This high-profit

margin allows us to mitigate price fluctuations related to factors such as energy consumption, catalyst costs, and production scale. Overall, the co-upcycling process of plastic offers advantages in terms of efficiency, greenhouse gas emissions, environmental impact, and economic benefit.

## Discussion

In conclusion, we developed a simple and highly efficient process for co-upcycling two commodity waste polymers, PC and PET, into a high-performance transparent engineering plastic (PAR). At relatively mild conditions, various end-of-life PC plastics and PET plastics/fabrics were

methanolysed over [TBDH]Ac catalysts to obtain r-BPA and r-DMT monomers with a purity of 98% and 99%, respectively. In contrast to conventional practices with additional purification to prepare highly pure monomers for re-polymerization, the recovered monomers could be directly used to prepare r-PAR using a two-stage interface polymerization technique with variable temperature control, minimizing the adverse effects of the existing impurities for re-polymerization. The r-PAR exhibits excellent thermal stability, high mechanical strength, and better melt flowability compared to a commercial PAR product, U-100. The recycling process supports operation on a large scale and could be employed to prepare PAR film material with excellent transparency, flexibility, transmittance, and flame retardancy. Through LCA analysis, we have shown that r-PAR produced through this co-upcycling approach could significantly reduce GWP (by at least 26%) and environmental impact in terms of freshwater ecotoxicity and human toxicity, in comparison to current waste management methods. This methodology substantially streamlines the process of upgrading and recycling waste PET and PC, resulting in reduced energy consumption and enabling large-scale industrial production of high-performance special engineering plastics from waste commodity polymers.

## Methods

### Polyester materials, chemicals, and reagents

Acetic acid (Ac, >99.5%, General-reagent), lactic acid (LA, 85–90%, Keshi), trifluoroacetic acid (TFA, 99%, Adamas), methanesulfonic acid (MSA, 99%, Adamas), 1,5,7-triazabicyclo[4.4.0]dec-5-ene (TBD, 99%, Adamas), 1,8-diazabicyclo[5.4.0]-7-undecene (DBU, 98%, Adamas), 7-methyl-1,5,7-triazabicyclo[4.4.0]dec-5-ene (MTBD, 99%, Adamas), tetrabutylammonium hydroxide (40 wt% in water, Adamas), 1-butyl-3-methylimidazolium acetate ([Bmim]Ac, 98%, Adamas), anhydrous methanol (99.9%, Adamas), diphenyl carbonate (DPC, 99%, Adamas), terephthaloyl acid chloride (TPC, 99.9%), isophthalic acid chloride (IPC, 99.9%, Qingdao Sanli Benzo New Material Co., Ltd) and bisphenol A (r-BPA) obtained from the recycled PC, chlormequat chloride (AR, Chengdu KeLong Chemical Industry Company), dichloromethane ( $\text{CH}_2\text{Cl}_2$ ), sodium hydroxide (NaOH) (AR, Chengdu Ke Long Chemical Industry Company), PC was purchased from Covestro (particle size 3 nm,  $M_w$  - 25,000–30,000), Mitsubishi (particle size 3 nm,  $M_w$  - 26,000) and Shanghai Macklin Biochemical (particle size 3 nm,  $M_w$  - 26,000), respectively.

### Procedures for the synthesis of ILs

Synthesis of [TBDH]Ac, [TBDH]LA, [TBDH]TFA, [TBDH]MSA, [TBDH]Cl, [DBUH]Ac, [MTBDH]Ac. Generally, protic ILs composed of cation and imidazole anions were one-step synthesized by acid-base neutralization reaction under ambient conditions. Typically, 5 mmol of TBD and 5 mL of  $\text{H}_2\text{O}$  were added to a 20 mL round-bottomed flask; equimolar Ac was slowly introduced with stirring. Then, the neutralization reaction was allowed to proceed at ambient temperature for 24 h. The white crystal [TBDH]Ac was obtained by rotating evaporation. These ILs were vacuum-dried for 48 h at 60 °C before use to remove any residual water.

Synthesis of [N<sub>4444</sub>]Ac by anion exchange method: In a typical experiment, 5 mmol of tetrabutylammonium hydroxide, 5 mL of  $\text{H}_2\text{O}$  and 5 mmol of Ac were mixed in a 20 mL round-bottomed flask, equipped with a magnetic stirring bar and sealed with a cap. The mixture was stirred at room temperature for 24 h. The crystal IL was obtained by rotating evaporation. The IL was vacuum-dried for 48 h at 60 °C before use to remove any residual water. Details on NMR information of ILs can be found in the Supplementary Information.

### Evaluation of catalytic methanolysis

The catalytic methanolysis of PC or PET was carried out in a 15 mL stainless-steel autoclave with magnetic stirring. In a typical procedure,

0.5 g of PC or PET ( $w_1$ ), 2 mL of MeOH, and 0.25 mmol of catalyst were transferred into the autoclave together. Then it was heated to 100 °C or 150 °C and kept for 2 h. After cooling, the obtained mixture was filtered and washed with methanol to obtain the residual PC or PET. The residual PC or PET was washed, dried at 70 °C for 12 h, and then weighed ( $w_2$ ) to calculate the conversion of PC or PET. The filtrate was concentrated, and the residue was extracted with ethyl acetate and deionized water. The r-BPA or r-DMT ( $w_3$ ) could be obtained from the organic phase by rotary evaporation. In the case of real plastics, the non-reactive substance ( $w_4$ ) remains, and its theoretical content is determined through repeated controlled experiment with extended reaction times of 24 h. The purity of the r-BPA and r-DMT was analyzed by  $^1\text{H}$  NMR. The conversion and yield were calculated using the following equations:

$$\text{PC conversion} = \frac{w_1 - w_2}{w_1 - w_4} \times 100\% \quad (1)$$

$$\text{r-BPA yield} = \frac{w_3 \times \text{Purity}_{\text{BPA}} \times M_{\text{PC}}}{M_{\text{BPA}} \times (w_1 - w_4)} \quad (2)$$

where  $M_{\text{PC}}$  and  $M_{\text{BPA}}$  are the molar mass of the PC unit and BPA.

$$\text{PET conversion} = \frac{w_1 - w_2}{w_1 - w_4} \times 100\% \quad (3)$$

$$\text{r-DMT yield} = \frac{w_3 \times \text{Purity}_{\text{DMT}} \times M_{\text{PET}}}{M_{\text{DMT}} \times (w_1 - w_4)} \quad (4)$$

where  $M_{\text{PET}}$  and  $M_{\text{DMT}}$  are the molar mass of the PET unit and DMT.

In the cyclic experiments, the recovered IL yield is about 90%. Due to the loss of IL (~0.1 eq of fresh IL) during the separation process, the amount of recovered ionic liquid was less than the feed amount. In the subsequent reaction cycles, 0.1 eq of fresh IL was added each time with the recycled ionic liquid.

### Polymer synthesis

In this study, the r-PAR was synthesized by a facile interfacial polymerization in the range of 5–18 °C. Take a typical example: r-BPA containing a small amount of end-capping agent (45.6 g, 0.2 mol), NaOH (16.2 g, 0.41 mol) and deionized water (280 mL) were added into a 1000 mL three-necked flask equipped with a mechanical stirrer and nitrogen inlet/outlet. After stirring for about 30 min at 5–10 °C in the dark, the butyltrimethylammonium chloride catalyst (0.5 g) was added into the flask. The mixture solution of IPC (20.3 g, 0.1 mol) and TPC (20.3 g, 0.1 mol) (dissolved in 200 mL dichloromethane) was added dropwise within 30 min. The polymerization reaction was kept at 5–10 °C for about 3–4 h, then the reaction temperature was raised up to 15–18 °C to conduct an end-capping reaction utilizing the residual capping agents from recycled BPA monomers. Then the viscous reaction mixture was pumped (with a peristaltic pump) into a 1 L solvent-recovery-unit which was filled with 60 °C water to recover the solvent dichloromethane and solidify the crude product. The collected crude product was pulverized and further washed with hot deionized water to yield r-PAR 71.3 g (yield: 99.6%).

### Characterization

Products were detected by Gas Chromatography-Mass Spectrometer (GC-MS, Thermo Scientific ISQ-7610), which used TG-5 MS (30 m × 0.25 mm × 0.25 μm) as a capillary column. The molecular weights (weight-average and number-average molecular weights) of polymers were obtained by HLC-8320 gel permeation chromatography (GPC) with THF as eluent. Inherent viscosity analysis: the inherent viscosities ( $\eta_{\text{inh}}$ ) of the polymers were characterized by a Cannon-Ubbelodhe viscosimeter using NMP as the solvent, and



calculated with Solomon-Ciuta equation as follows:

$$\eta_{inh} = \frac{\sqrt{2(\eta_{sp} - \ln \eta_r)}}{C} \quad (5)$$

where  $\eta_r = t/t_0$ ,  $\eta_{sp} = t/t_0 - 1$ , where  $t$  is the solution flow time (s),  $t_0$  is the solvents (NMP) flow time (s),  $C$  is the solution concentration (g dl<sup>-1</sup>). Chemical structure analysis: The FT-IR test was recorded on a Nicolet NEXUS 670 spectrophotometer. <sup>1</sup>H-NMR and <sup>13</sup>C-NMR test was recorded on a 600 MHz Bruker spectrometer using deuterated dimethyl sulfoxide (DMSO-d<sub>6</sub>) or deuterated chloroform (CDCl<sub>3</sub>) as solvent. Thermal analysis: thermal characterization of these samples was performed with DSC (Mettler Toledo DSC3) and TGA (TGA Q500 V6.4 Build 193 thermal analysis instrument). The stress-strain behavior was tested on the MTS E45 electronic universal testing machine. The stretch spline size was length × width × depth = 5 cm × 0.4 cm × (0.15–0.3) cm. The load speed of tests was 2 mm min<sup>-1</sup>. Each value was obtained from the average results of 5 specimens. The thickness of the film is about 10–12 μm. The rheological properties were tested by Bohlin Gemini 200 and TA AR-G2 parallel plate rheometer (temperature scanning: 280–320 °C, time scanning: 0–1800 s (300 and 310 °C), frequency: 1 Hz).

### Life-cycle assessment

The LCA analysis followed the ISO standard series 14040 and 14067. Data used to build the life-cycle inventory were collected from scale-up experimental and the commercial database Ecoinvent 3.7. Identify the feasibility of upcycling PC and PET to PAR design and compare the results to virgin PC, virgin PET, and other recovery methods. The system boundary is cradle-to-grave, and the whole process of depolymerization included the production or re-polymerization of PC, PET, and PAR, the collection and transportation of waste plastic. Nine environmental impact categories were assessed, namely climate change (GWP) and human toxicity, cancer effects (HT-cancer), etc. The detailed data and assumptions can be found in Supplementary Information.

### Data availability

The experiment data generated in this study are provided in Supplementary Information. Source data is available from the corresponding author upon request.

### References

- Vidal, F. et al. Designing a circular carbon and plastics economy for a sustainable future. *Nature* **626**, 45–57 (2024).
- Ma, D. Transforming end-of-life plastics for a better world. *Nat. Sustain.* **6**, 1142–1143 (2023).
- Plastics – the fast Facts 2023, <https://plasticseurope.org/wp-content/uploads/2023/10/Plasticsthefastfacts2023-1.pdf>
- Zhang, F. et al. From trash to treasure: chemical recycling and upcycling of commodity plastic waste to fuels, high-valued chemicals and advanced materials. *J. Energy Chem.* **69**, 369–388 (2022).
- Ellis, L. D. et al. Chemical and biological catalysis for plastics recycling and upcycling. *Nat. Catal.* **4**, 539–556 (2021).
- Lee, K., Jing, Y. X., Wang, Y. Q. & Yan, N. A unified view on catalytic conversion of biomass and waste plastics. *Nat. Rev. Chem.* **6**, 635–652 (2022).
- Schechter, A. et al. Bisphenol A (BPA) in U.S. food. *Environ. Sci. Technol.* **44**, 9425–9430 (2010).
- Schwab, S. T., Baur, M., Nelson, T. F. & Mecking, S. Synthesis and deconstruction of polyethylene-type materials. *Chem. Rev.* **124**, 2327–2351 (2024).
- Zhang, F. et al. Polyethylene upcycling to long-chain alkylaromatics by tandemhydrogenolysis/aromatization. *Science* **370**, 437–441 (2020).
- Vogt, E. T. C. & Weckhuysen, B. M. The refinery of the future. *Nature* **629**, 295–306 (2024).
- Jing, Y. X. et al. Towards the circular economy: converting aromatic plastic waste back to arenes over a Ru/Nb<sub>2</sub>O<sub>5</sub> catalyst. *Angew. Chem. Int. Ed.* **60**, 5527–5535 (2021).
- Li, Y. W. et al. Catalytic transformation of PET and CO<sub>2</sub> into high-value chemicals. *Angew. Chem. Int. Ed.* **61**, e202117205 (2022).
- Sullivan, K. P. et al. Mixed plastics waste valorization through tandem chemical oxidation and biological funneling. *Science* **378**, 207–211 (2022).
- Wei, J. D. et al. Hydrodeoxygenation of oxygen-containing aromatic plastic wastes to liquid organic hydrogen carriers. *Angew. Chem. Int. Ed.* **62**, e20231050 (2023).
- Jiang, T.-W. et al. Recycling waste polycarbonate to bisphenol A-based oligoesters as epoxy-curing agents, and degrading epoxy thermosets and carbon fiber composites into useful chemicals. *ACS Sustain. Chem. Eng.* **10**, 2429–2440 (2022).
- Si, G. F., Li, C., Chen, M. & Chen, C. L. Polymer multi-block and multi-block<sup>+</sup> strategies for the upcycling of mixed polyolefins and other plastics. *Angew. Chem. Int. Ed.* **62**, e2023117 (2023).
- Zhang, D., Wang, X., Zhang, Z. B. & Hadjichristidis, N. Heteroatom substitution strategy modulates thermodynamics towards chemically recyclable polyesters and monomeric unit sequence by temperature switching. *Angew. Chem. Int. Ed.* **63**, e202402233 (2024).
- Cao, X. H., Zhang, W. D., Wang, X. & Zhang, Z. B. A γ-butyrolactone-derived poly(vinyl ester) with pendant groups recyclability and controlled release of poly(vinyl alcohol): Synthesis, recyclability, and physical properties. *Reactive Funct. Polymers* **175**, 105269 (2022).
- Wang, Y. C., Zhu, Y. N., Lv, W. X., Wang, X. H. & Tao, Y. H. Tough while recyclable plastics enabled by monothiodilactone monomers. *J. Am. Chem. Soc.* **145**, 1877–1885 (2023).
- Manker, L. P. et al. Performance polyamides built on a sustainable carbohydrate core. *Nat. Sustain.* **7**, 640–651 (2024).
- Coates, G. W. & Getzler, Y. D. Y. L. Chemical recycling to monomer for an ideal, circular polymer economy. *Nat. Rev. Mater.* **5**, 501–516 (2020).
- Qin, B. et al. Closed-loop chemical recycling of cross-linked polymeric materials based on reversible amidation chemistry. *Nat. Commun.* **13**, 7959 (2022).
- Fan, L. X. et al. Dual photo-responsive diphenylacetylene enables PET in-situ upcycling with reverse enhanced UV-resistance and strength. *Angew. Chem. Int. Ed.* **62**, e202314448 (2023).
- Jones, G. O. et al. Computational and experimental investigations of one-step conversion of poly(carbonate)s into value-added poly(aryl ether sulfone)s. *Proc. Natl. Acad. Sci. USA* **113**, 7722–7726 (2016).
- Zhang, X., Guo, W. Q., Zhang, C. J. & Zhang, X. H. A recyclable polyester library from reversible alternating copolymerization of aldehyde and cyclic anhydride. *Nat. Commun.* **14**, 5423 (2023).
- Wu, F. T. et al. Lactate anion catalyzes aminolysis of polyesters with anilines. *Sci. Adv.* **9**, eade7971 (2023).
- Xu, Y. L. et al. Polymeric carbon nitride nanosheets as a metal-free heterogeneous catalyst for highly efficient methanolysis of polycarbonates. *ChemCatChem* **16**, e202301763 (2024).
- Jehanno, C. et al. Selective chemical upcycling of mixed plastics guided by a thermally stable organocatalyst. *Angew. Chem. Int. Ed.* **60**, 6710–6717 (2021).
- Wu, C.-H., Chen, L.-Y., Jeng, R.-J. & Dai, S. A. 100% Atom-economy efficiency of recycling polycarbonate into versatile intermediates. *ACS Sustain. Chem. Eng.* **6**, 8964–8975 (2018).
- Jehanno, C. et al. Critical advances and future opportunities in upcycling commodity polymers. *Nature* **603**, 803–814 (2022).
- Wang, J. et al. Promoting aromatic hydrocarbon formation via catalytic pyrolysis of polycarbonate wastes over Fe- and Ce-loaded aluminum oxide catalysts. *Environ. Sci. Technol.* **54**, 8390–8400 (2020).

32. Zhang, S. B. et al. Depolymerization of polyesters by a binuclear catalyst for plastic recycling. *Nat. Sustain.* **6**, 965–973 (2023).
33. Wu, F. T. et al. Upcycling poly(succinates) with amines to N-substituted succinimides over succinimide anion-based ionic liquids. *Nat. Commun.* **15**, 712 (2024).
34. Qin, B. & Zhang, X. On depolymerization. *CCS Chem.* **6**, 297–312 (2024).
35. Ahrens, A. et al. Catalytic disconnection of C–O bonds in epoxy resins and composites. *Nature* **617**, 730–737 (2023).
36. Shi, C. X., Quinn, E. C., Diment, W. T. & Chen, E. Y. X. Recyclable and (bio)degradable polyesters in a circular plastics economy. *Chem. Rev.* **124**, 4393–4478 (2024).
37. Clark, R. A. & Shaver, M. P. Depolymerization within a circular plastics system. *Chem. Rev.* **124**, 2617–2650 (2024).
38. Bhowmik, P. K. & Han, H. Fully aromatic liquid-crystalline polyesters of phenyl-substituted 4,4'-biphenols and 1,1'-binaphthyl-4,4'-diol with either 2-bromoterephthalic acid. *Macromolecules* **26**, 5287–5294 (1993).
39. Zhang, Y., Yan, G.-m., Zhang, G., Liu, S.-L. & Yang, J. Synthesis of high transparency polyarylates containing cyclohexane group. *Polymer* **186**, 122047 (2020).
40. Wang, Z. F., Liu, Y. Y., Wang, B. L., Long, X. B. & Yao, W. L. Synthesis and properties of novel block-structured polyarylates containing fluorene: a two-step interface polymerization. *New. J. Chem.* **48**, 10497–10506 (2024).
41. Liu, F. S. et al. Environmentally benign methanolysis of poly-carbonate to recover bisphenol A and dimethyl carbonate in ionic liquids. *J. Hazard. Mater.* **174**, 872–875 (2010).
42. Liu, M. Y. et al. Transformation of alcohols to esters promoted by hydrogen bonds using oxygen as the oxidant under metal-free conditions. *Sci. Adv.* **4**, eaas9319 (2018).
43. Qu, X. L. et al. Synergistic catalysis of imidazole acetate ionic liquids for the methanolysis of spiral poly(ethylene 2,5-furandicarboxylate) under a mild condition. *Green Chem.* **23**, 1871–1882 (2021).
44. Liu, Y. C. et al. Degradation of poly(ethylene terephthalate) catalyzed by metal-free choline-based ionic liquids. *Green Chem.* **22**, 3122–3131 (2020).
45. Gross, S. M., Roberts, G. W., Kiserov, D. J. & DeSimone, J. M. Synthesis of high molecular weight polycarbonate by solid-state polymerization. *Macromolecules* **34**, 3916–3920 (2001).
46. Koda, H., Megumi, T., & Yoshizaki, H. Process for producing polycarbonate oligomers. *US Patent* 4122112, published on October 24 (1978).
47. Nishino, K., Shindo, Y., Takayama, T. & Ito, H. Improvement of impact strength and hydrolytic stability of PC/ABS blend using reactive polymer. *J. Appl. Polym. Sci.* **134**, 44550 (2017).
48. Chen, L., Zhao, D., Wang, X.-L. & Wang, Y.-Z. Durable macro-molecular firefighting for unsaturated polyester via integrating synergistic charring and hydrogen bond. *Chem. Eng. J.* **443**, 136365 (2022).
49. Dastidar, R. G. et al. Catalytic production of tetrahydropyran (THP): a biomass-derived, economically competitive solvent with demonstrated use in plastic dissolution. *Green Chem.* **24**, 9101–9113 (2022).
50. Li, H. Q. et al. Hydroformylation of pyrolysis oils to aldehydes and alcohols from polyolefin waste. *Science* **381**, 660–666 (2023).

## Acknowledgements

This work was financially supported by the National Key R&D Program of China (2023YFC3903200), National Science Foundation of China (22272114, 22078204), Science and Technology Program of Sichuan Province (2023ZYD0029), Fundamental Research Funds from Sichuan University (2022SCUNL103, 2023SCUH0004) and the Project of State Key Laboratory of Polymer Materials Engineering at Sichuan University (sklpme2020-3–11). We thank Prof. Yuzhong Wang from the National Engineering Laboratory of Eco-Friendly Polymeric Materials of Sichuan University for his guidance and suggestions on the project.

## Author contributions

F.Z. and G.Z. conceived the project and designed the experiments. C.L., G.Y., and Z.D. performed most of the experiments. C.L., G.Y., G.Z., and F.Z. collaboratively analyzed the data and wrote the paper. All authors contribute to the discussion and revision of the paper.

## Competing interests

The authors declare no competing interests.

## Additional information

**Supplementary information** The online version contains supplementary material available at <https://doi.org/10.1038/s41467-025-57821-7>.

**Correspondence** and requests for materials should be addressed to Gang Zhang or Fan Zhang.

**Peer review information** *Nature Communications* thanks Meidong Lan, Jiwoong Lee and Lopez de Pariza for their contribution to the peer review of this work. A peer review file is available.

**Reprints and permissions information** is available at <http://www.nature.com/reprints>

**Publisher's note** Springer Nature remains neutral with regard to jurisdictional claims in published maps and institutional affiliations.

**Open Access** This article is licensed under a Creative Commons Attribution-NonCommercial-NoDerivatives 4.0 International License, which permits any non-commercial use, sharing, distribution and reproduction in any medium or format, as long as you give appropriate credit to the original author(s) and the source, provide a link to the Creative Commons licence, and indicate if you modified the licensed material. You do not have permission under this licence to share adapted material derived from this article or parts of it. The images or other third party material in this article are included in the article's Creative Commons licence, unless indicated otherwise in a credit line to the material. If material is not included in the article's Creative Commons licence and your intended use is not permitted by statutory regulation or exceeds the permitted use, you will need to obtain permission directly from the copyright holder. To view a copy of this licence, visit <http://creativecommons.org/licenses/by-nc-nd/4.0/>.

© The Author(s) 2025